Grenze International Journal of Engineering and Technology, Jan Issue

SSR Mitigation in Power System by LQR Control of nearby DFIG

Dr. Nilaykumar A. Patel[1] and Khush N. Patel[2]
[1-2]Dept. of Electrical Engineering, CSPIT-CHARUSAT UNIVERSITY, Changa, Gujarat, India
Email: nilaypatel.ee@charusat.ac.in, patelkp2002@gmail.com

***Abstract*— This study examines the influence of a direct-power control technique for a DFIG (Doubly-Fed Induction Generator)-based wind generator on sub-synchronous resonance (SSR). A series capacitor of a transmission line will exchange power with the synchronous generator when it runs via an SSR. DFIG includes power converters built into its rotor circuit, allowing for quick control of both the active and reactive power of the device. This is made possible by the rotor converter circuit's fast IGBT switching. Examining the ability of the LQR (Linear Quadratic Regulator) on the DFIG to provide the required active power and reactive power during SSR is the primary goal of this work. Additional DFIG is added to the test system in addition to the original test system, and during SSR its performance is evaluated using an additional control signal that is obtained from the synchronous generator and supplied to DFIG through LQR. The analysis of SSR was completed based on eigenvalue analysis utilizing the D-Q model test system and transient simulation using MATLAB Simulink. Independent model control is used to control the DFIG rotor converter that dampens multimodal SSR oscillations. The test system was developed using the IEEE first benchmark model's adopted system.**

***Index Terms*— Subsynchronous resonance, Linear Quadratic Regulator, DFIG, IEEE First Benchmark Model, Eigenvalue Analysis, Rotor side converter control.**

I. INTRODUCTION

In order to combat the line reactance effect on scarcely accessible transmission lines, utilities are forced to employ series capacitors due to the rapidly exponentially increasing development of electrical power consumption. Due to negative damping, however, this series of capacitors will be crucial in causing subsynchronous oscillation in the mass-spring system of the generator and turbine [1], [2]. The shaft torque may be magnified as a result of brief disruptions. Two consecutive shaft failures caused by torsional SSR oscillations happened in 1970 and 1971 at the Mohave power plant in the US, according to reports of this kind of incidence [3, 4]. Numerous solutions, including the employment of FACTS devices TCSC [5], SSSC [6], and SVC [7], excitation voltage control [8], modified power system stabilizers [9], and interplant power-flow controllers [10], have been suggested to prevent these types of accidents. It has also been noted in [11] that power control over additional DFIG can reduce SSR. Many of the recommended solutions can successfully reduce one oscillation mode but fall short in their ability to suppress additional oscillation modes that develop as a result of various levels of series compensation. As a result, one's thoughts should be directed toward finding a source that is appropriate and capable of providing the necessary level of power. Numerous academic works propose direct power regulation of the DFIG, which provides excellent transient responsiveness. With one modification, the IEEE FBM, the first benchmark modal, is employed here as

Grenze ID: 01.GIJET.10.1.11

the test system. To enable the mitigation of SSR in the test system, one additional DFIG with LQR is added into the test system provided in IEEE FBM. The power converter's quick control features and LQR control make the DFIG the best option for providing the necessary power to suppress SSR. According to the diverse publications, a stator flux-oriented vector control is the most widely used technique. [12]- [14]. Variations between the system's actual parameters and their actual values have an impact on the system's performance. Even when parameters are changed, the direct power control method in the absence of rotor current [15] provides a stable response. The work's main goal is to evaluate how well the DFIG's new direct active and reactive power control along with LQR works to reduce subsynchronous oscillations. The synchronous generator load angle was used to generate one input signal that was provided to the DFIG control circuit and LQR.

The paper is structured as follows: Section II provides a description of the test system. Section III provides a mathematical model of the improved IEEE FBM test system for SSR in the D-Q frame. The controller design description, the IEEE FBM test system for SSR, and the DFIG power control scheme are provided in Section IV. Simulation results and their discussion are reported in Section V, and conclusions are presented in Section VI.

II. TEST SYSTEM

Figure 1 shows the single-line diagram of the test system. With the exception of the DFIG, the test system in the aforementioned picture follows the IEEE's first benchmark model for SSR research. Since we will be controlling the power of the DFIG, which has a total of three masses in the test system, it is regarded as a single-mass model. Due to its modeling approach, DFIG will only take part in network mode. The resonance probabilities observed in this case are consistent with those of the original IEEE FBM (First Benchmark Model) system. The generator may be conceptualized as an assemblage of generators that have a common mechanical design. The DFIG seen in Fig. 1 might perhaps originate from a nearby wind power facility or have been recently installed in close proximity to the original producing station. The system's loading is chosen to prevent the transformer from becoming overloaded.

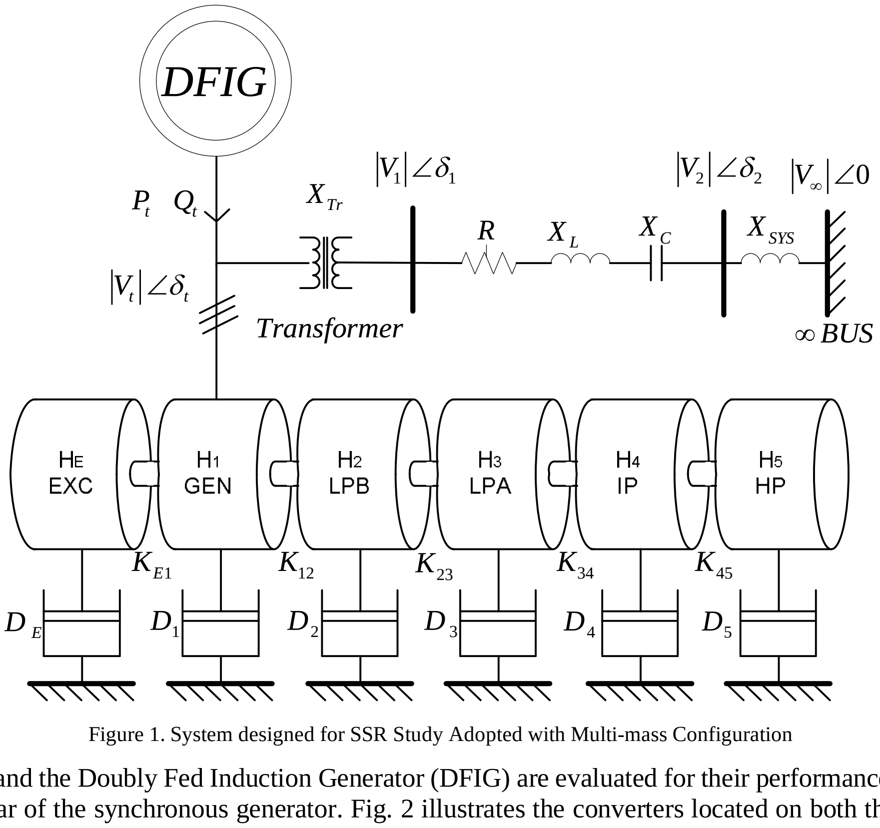

Figure 1. System designed for SSR Study Adopted with Multi-mass Configuration

The controller and the Doubly Fed Induction Generator (DFIG) are evaluated for their performance by connecting them to a busbar of the synchronous generator. Fig. 2 illustrates the converters located on both the grid-side and rotor-side of the Doubly Fed Induction Generator (DFIG). The transformer is supplied with regulated electricity prior to being supplied to the power system. During subsynchronous oscillations, the LQR control strategy for DFIG rotor converters is designed to prevent the mechanical mass system of the synchronous generator from experiencing subsynchronous resonance with the series capacitor of the transmission line.

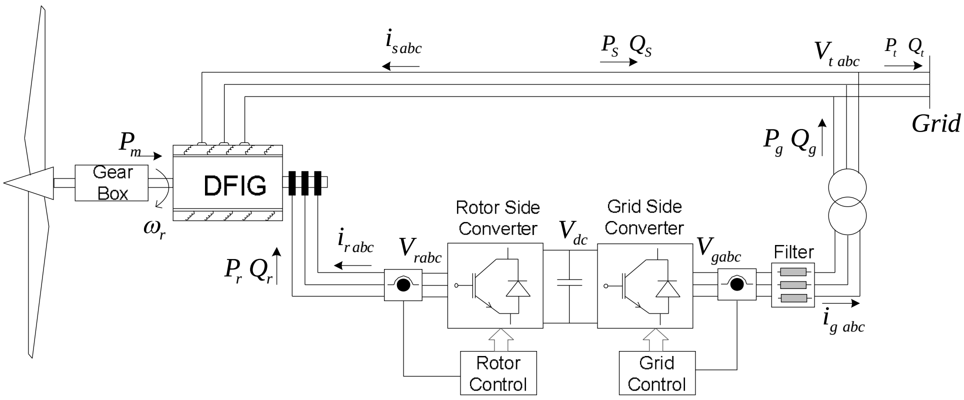

Figure 2. Wind Energy Conservation System by DFIG

III. Modeling Of Test System

A. Modeling of DFIG for SSR Control

The Doubly Fed Induction Generator (DFIG) has resemblance to a wound rotor induction generator. It incorporates a direct current (DC) connection between the back-to-back converters, which are sustained by a capacitor bank. Additionally, the rotor circuit is linked to the grid through the converters. The quick-acting IGBTs allow for quick output power regulation in both directions via the rotor circuit. As a result, control over SSR can be performed by operating the DFIG at either subsynchronous or super-synchronous speed. The voltage and flux equations for DFIG in both D-Q form and in any reference frame are,

$$\left.\begin{aligned} v_{ds} &= p\psi_{ds} - \omega\psi_{qs} + R_s i_{ds} \\ v_{qs} &= p\psi_{qs} + \omega\psi_{ds} + R_s i_{qs} \end{aligned}\right\} \tag{1}$$

$$\left.\begin{aligned} v_{dr} &= p\psi_{dr} - (\omega - \omega_r)\psi_{qr} + R_s i_{dr} \\ v_{qr} &= p\psi_{qr} + (\omega - \omega_r)\psi_{dr} + R_s i_{qr} \end{aligned}\right\} \tag{2}$$

$$\left.\begin{aligned} \psi_{ds} &= L_m i_{dr} + L_s i_{ds} \\ \psi_{qs} &= L_m i_{qr} + L_s i_{qs} \end{aligned}\right\} \tag{3}$$

$$\left.\begin{aligned} \psi_{dr} &= L_r i_{dr} + L_m i_{ds} \\ \psi_{qr} &= L_r i_{qr} + L_m i_{qs} \end{aligned}\right\} \tag{4}$$

Where the currents flowing in stator and rotor are , the flux linkages are , the speed of DFIG is , the resistance of stator winding and the resistance of rotor winding are Rs and Rr respectively.

The matrix form of the aforementioned equations under the synchronous reference frame will be as follows:

$$\begin{bmatrix} v_{ds}^e \\ v_{qs}^e \end{bmatrix} = \begin{bmatrix} L_s p & -\omega_s L_s \\ \omega_s L_s & L_s p \end{bmatrix} \begin{bmatrix} i_{ds}^e \\ i_{qs}^e \end{bmatrix} + L_m \begin{bmatrix} p & -\omega_s \\ \omega_s & p \end{bmatrix} \begin{bmatrix} i_{dr}^e \\ i_{qr}^e \end{bmatrix} \tag{5}$$

$$\begin{bmatrix} v_{dr}^e \\ v_{qr}^e \end{bmatrix} = \begin{bmatrix} R_r + L_r p & -s\omega_s L_r \\ s\omega_s L_r & R_r + L_s p \end{bmatrix} \begin{bmatrix} i_{dr}^e \\ i_{qr}^e \end{bmatrix} + L_m \begin{bmatrix} p & -s\omega_s \\ s\omega_s & p \end{bmatrix} \begin{bmatrix} i_{ds}^e \\ i_{qs}^e \end{bmatrix} \tag{6}$$

Where e stands for the synchronous reference frame and s for the slip. Next, using “(5)”,

$$\begin{bmatrix} i_{ds}^e \\ i_{qs}^e \end{bmatrix} = \frac{1}{L_s\left(p^2 + \omega_s^2\right)} \begin{bmatrix} p & \omega_s \\ -\omega_s & p \end{bmatrix} \left\{ \begin{bmatrix} v_{ds}^e \\ v_{qs}^e \end{bmatrix} - L_m \begin{bmatrix} p & -\omega_s \\ \omega_s & p \end{bmatrix} \begin{bmatrix} i_{dr}^e \\ i_{qr}^e \end{bmatrix} \right\} \tag{7}$$

The equation of the transients in rotor voltages in synchronous reference frame for the DFIG can be obtained using “(6)” and “(7)”,

$$\begin{bmatrix} v_{dr}^e \\ v_{qr}^e \end{bmatrix} = \begin{bmatrix} R_r + L_r^{'} p & -s\omega_s L_r^{'} \\ s\omega_s L_r^{'} & R_r + L_r^{'} p \end{bmatrix} \begin{bmatrix} i_{dr}^e \\ i_{qr}^e \end{bmatrix} + D \cdot \begin{bmatrix} v_{ds}^e \\ v_{qs}^e \end{bmatrix} \quad (8)$$

The rotor transient inductance is denoted by $L_r^{'}$, $L_r^{'} = \sigma L_r$ where $\sigma = 1 - L_m^2 / (l_s L_r)$ and

$$D = \frac{L_m}{L_s} \frac{1}{p^2 + \omega_s^2} \begin{bmatrix} p^2 + s\omega_s^2 & (1-s)\omega_s p \\ (s-1)\omega_s p & p^2 + s\omega_s^2 \end{bmatrix} \quad (9)$$

The active and reactive powers of DFIG are found as under,

$$P_s = \frac{3}{2}\left(v_{ds} i_{ds} + v_{qs} i_{qs}\right) = -\frac{3}{2} \frac{L_m}{L_s} v_{qs} i_{qr} \quad (10)$$

$$Q_s = \frac{3}{2}\left(v_{qs} i_{ds} - v_{ds} i_{qs}\right) = \frac{3}{2} v_{qs} \left(\frac{L_m}{L_s} i_{dr} - \frac{v_{qs}}{\omega_s L_s} \right) \quad (11)$$

By installing an SVC-type device, the terminal voltage may be maintained constant, and rotor currents can be used to manage the stator's active and reactive power.

B. Modeling of Synchronous Machine

Here, the state-space equations developed from the test system's D-Q modeling are used [16]. Linearized equations around the operating point are generated in order to do eigenvalue analysis. The state-space matrix is created together with the linearized equations for the turbine-generator mass system with a series capacitor. Fig. 1 depicts the generator's rotor model.

The synchronous generator is a type 2.2 model of the synchronous machine. Three-phase winding is on the stator; the rotor is wound with a field winding and the position of damper winding is on the D axis, and other two damper windings are located on the Q axis, whereas the stator has three phases of winding. This approach uses detailed models to accurately depict the rotor's motions. The following fundamental equations can be used to obtain the space-state equations for each generator.

$$\psi_s = \left[L_{ss}\right] i_s + \left[L_{sr}\right] i_r \quad (12)$$

$$\psi_r = \left[L_{rs}\right] i_s + \left[L_{rr}\right] i_r \quad (13)$$

The matrices of rotor and stator self as well as mutual inductance are used in the aforementioned equations. The aforementioned equations are changed to a D-Q reference frame, and after that, linearized.

C. Modeling of Multi-Mass Turbine-Generator Set

One generator mass stage, one exciter stage, and four turbine mass stages are used to illustrate the mechanical turbine-generator system in Fig. 1. Five soft steel shafts connect the six turbo generator masses, each of which has a different inertia. The following shaft torque equations are provided.

$$\left[2H\right] p^2 \underline{\delta} + \left[D\right] p \underline{\delta} + \left[K\right] \underline{\delta} + \underline{T} = 0 \quad (14)$$

The shaft stiffness matrix is indicated by [K], while [H] is representing the diagonal matrix of inertia and [D] represents the diagonal matrix of the damping coefficients. The resulting angular position vector is produced by the torque vector T operating on the shaft end. Damping is not considered in this paper. The speed and angular displacement from the reference line of each mass are the state variables taken into account.
The state matrix A for both generators may be obtained from “(14)”, and the eigenvalues are obtained as solution of the A matrix. With the help of the eigenvalues, the natural frequencies of the multi-mass model can be determined and are shown in table 1 below.

TABLE I. MODES OF SYSTEM AND THEIR CORRESPONDING FREQUENCY

Mode	0	1	2	3	4	5
Natural frequency (Hz)	1.66	15.73	20.23	25.50	32.37	47.31

D. Modeling of Electric Network

Fig. 3 illustrates the analogous electrical circuit used in the Institute of Electrical and Electronics Engineers (IEEE) Frequency-Based Method (FBM) for the purpose of investigating Sub-Synchronous Resonance (SSR). The connection between the generator, which has a constant voltage source (Eg) and terminal voltage (Vt), and an infinite bus is established through a series-compensated transmission line. The state equations for the d-q components of the electrical network are shown in “(15)” and “(16)”.

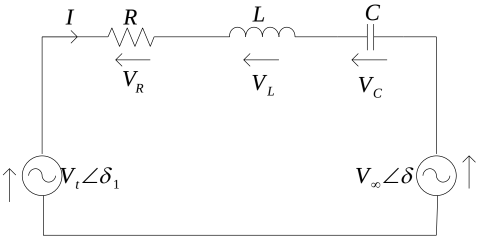

Figure 3. Electric Network Test System Model

$$\left.\begin{aligned} V_{td} &= Ri_d + \frac{X_L}{\omega_0} pi_d - \frac{\omega}{\omega_0} X_L i_q + v_{cd} + V_\infty \sin\delta \\ V_{tq} &= Ri_q + \frac{X_L}{\omega_0} pi_q + \frac{\omega}{\omega_0} X_L i_d + v_{cq} + V_\infty \cos\delta \end{aligned}\right\} \tag{15}$$

$$\left.\begin{aligned} pv_{cd} &= \omega v_{cq} + \omega_0 X_C i_d \\ pv_{cq} &= -\omega v_{cd} + \omega_0 X_C i_q \end{aligned}\right\} \tag{16}$$

IV. CONTROLLER DESIGN

A. Feedback Signal Selection

Optimal damping during the SSR state following a significant event, such as loss of a crucial line or a fault, is the goal of building an LQR. By permitting a larger range of operation, a properly built damping controller allows the synchronous generator and DFIG combination in the system to transmit power at an expanded limit.

With reference signals which can modify the active and reactive power of DFIG, which is situated at the generator terminal, it is first important to evaluate the modal controllability. We'll concentrate on the modes where DFIG exhibits strong controllability. The modes of interest should be easily observable in the chosen feedback output signal. In order to sort the available signals, the analysis of modal observability is evaluated. For the sake of simplicity, this analysis solely considers the generator speed deviations as available signals.

B. Power Control Scheme of DFIG

In the proposed control methodology, the direct axis of the synchronous reference frame remains stationary with respect to the stator flux. The stator resistance's influence may be disregarded and the stator flux can be kept at a constant level due to the direct connection of the stator to the grid. The stator voltage vector for a synchronous frame is given by “(1)” as,

$$v_{qs} = \omega_s \psi_{ds} \tag{17}$$

Equations (10) and (11) can be used to calculate the stator active and reactive power because the coefficient of power for a wind turbine is always kept at its ideal value.

$$\left.\begin{aligned} P_s &= -k_\sigma \omega_s \psi_{ds}^{\omega} \psi_{qr}^{\omega} \\ Q_s &= k_\sigma \omega_s \psi_{ds}^{\omega} \left(\frac{L_r}{L_m} \psi_{ds}^{\omega} - \psi_{dr}^{\omega} \right) \end{aligned}\right\} \tag{18}$$

where $k_\sigma = 1.5 L_m / \left(\sigma L_s L_r \right)$

The pair of equations shown below represents the necessary adjustments in the active power P and the reactive power Q to effectively control the oscillations of the rotor in a synchronous generator within a short timeframe, assuming that the stator flux stays constant.

$$\left.\begin{aligned}\Delta P_s &= -k_\sigma \omega_s \psi_{ds}^{\omega} \Delta \psi_{qr}^{\omega} \\ \Delta Q_s &= -k_\sigma \omega_s \psi_{ds}^{\omega} \Delta \psi_{dr}^{\omega}\end{aligned}\right\} \tag{19}$$

The rotor voltage needed to control power is obtained by solving “(8)”, “(18)”, and “(19)” and ignoring the rotor resistance.

$$\left.\begin{aligned}v_{dr}^{\omega} &= \left(K_{P_Q} + \frac{K_{I_Q}}{s}\right)\left(Q_s - Q_s^*\right) + \omega_{sl}\frac{P_s}{k_\sigma \omega_s \psi_{ds}^{\omega}} \\ v_{qr}^{\omega} &= \left(K_{P_P} + \frac{K_{I_P}}{s}\right)\left(P_s - P_s^*\right) + \omega_{sl}\left(\frac{L_r}{L_S}\psi_{ds}^{\omega} - \frac{Q_s}{k_\sigma \omega_s \psi_{ds}^{\omega}}\right)\end{aligned}\right\} \tag{20}$$

Fig. 4 depicts the schematic control diagram, in which the signal from the synchronous generator is used. The DFIG will use a signal to make up for the power exchanged by the synchronous generator during subsynchronous resonance. Only when the signal is in subsynchronous resonance will it become active.

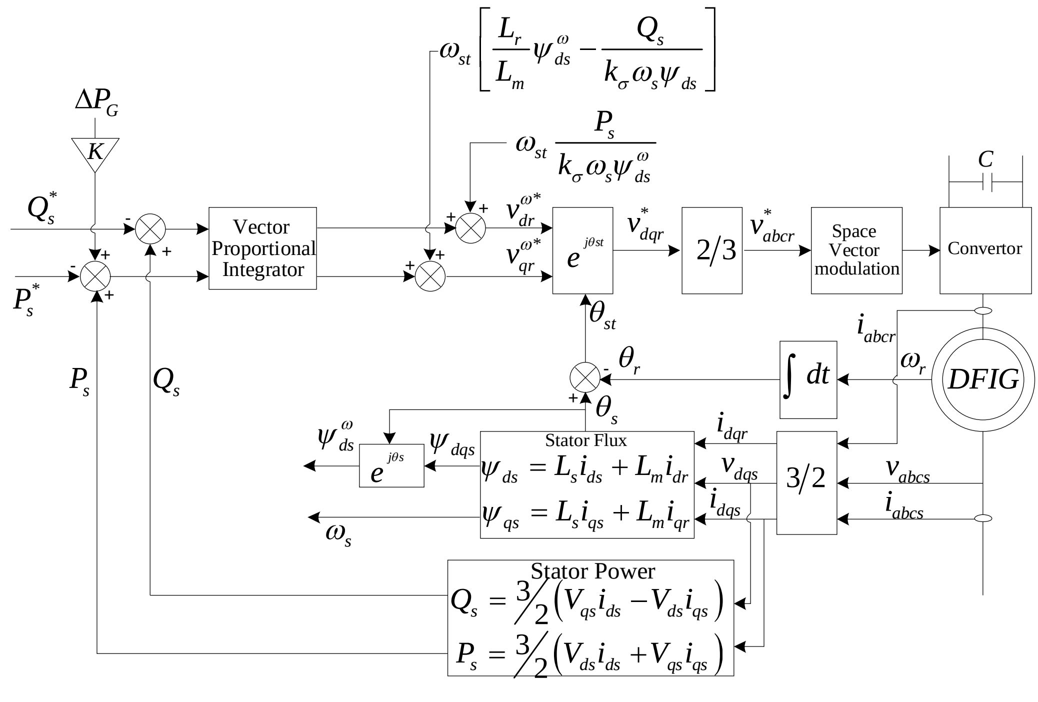

Figure 4. Block diagram of the control scheme for DFIG

C. Control Design Based on LQR

The representation of the state space linearized model of power system can be done in the following form:

$$\dot{x} = Ax + Bu + \Gamma w$$

$$y = Cx + v$$

where u is an input vector of m dimensions, y is an output vector of q dimensions, and x is an n-dimensional state vector. A stringent correct, linear, time-invariant, controlled, and observable plant is what is presumptively assumed. Additionally, w and v are the presumed uncorrelated white Gaussian noise and sensor error-noise inputs, respectively, with known covariance matrices V and W [15]. Fig. 5 illustrates the LQR control configuration.

The following quadratic cost function J can be minimized by selecting an optimal control input u, that is obtained using the LQR control method:

$$J = \lim_{T\to\infty} \frac{1}{T} E\int_0^T \left(z^T Qz + u^T Ru\right) dT \qquad (21)$$

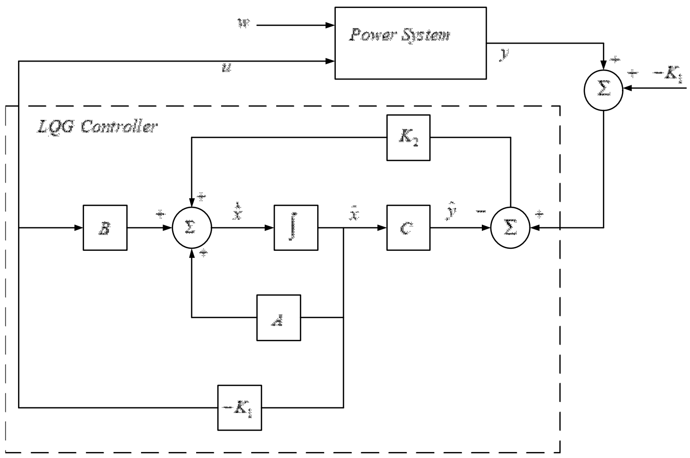

Figure 5. LQR Controller diagram

where either x or linear mixture of the states can be represented by z. $R^T = R \geq 0$ and $Q^T = Q \geq 0$ are achieved by carefully selecting the weighting parameters for the matrices Q and R. Both are often diagonal matrices. The best state feedback control law given by is computed using the reduced order system by:

$$u = -K_1 x \qquad (22)$$

Where $K_1 = R^{-1}B^T S$ and Ricatti equation's solution is obtained in form of S which is a unique symmetric semidefinite solution:

$$A^T S + SA + Q - SR^{-1}B^T S = 0 \qquad (23)$$

subject to [A] and [B] being stabilizable, R > 0, and [A], [Q] has no unobservable modes on the imaginary axis. Since it is impossible to measure every state of a plant, an estimator (Kalman filter) is used to extract the necessary estimations of the states from the accessible or measured outputs. The Kalman filter has the same structure as a standard state estimator, including:

$$\dot{\hat{x}} = A\hat{x} + Bu + K_2\left(y - C\hat{x}\right) \qquad (24)$$

where K2 is the Kalman filter gain which minimizes $J_f = E\left\{\left[x-\hat{x}\right]^T\left[x-\hat{x}\right]\right\}$, and is represented by:

$$K_2 = P_f C^T V^{-1} \qquad (25)$$

and the solution to the algebraic Ricatti equation is denoted as Pf, which is a unique symmetric positive semidefinite matrix.:

$$P_f A^T + AP_f - P_f C^T V^{-1} CP_f + \Gamma W \Gamma^T = 0 \qquad (26)$$

subject to [C] and [A] being detectable, $W \geq 0$, V > 0 and for $\left(A, \Gamma W \Gamma^T\right)$, there are no unmanageable modes present along the imaginary axis. Finally, the optimum control rule inside the Linear Quadratic Regulator (LQR) formulation is obtained as:

$$u = -K_1 \hat{x} \qquad (27)$$

Figure 6 depicts the suggested Linear Quadratic Regulator-based Power Oscillation Damping Controller (LQR-POD), which makes use of synchronous generator oscillations that have been measured.

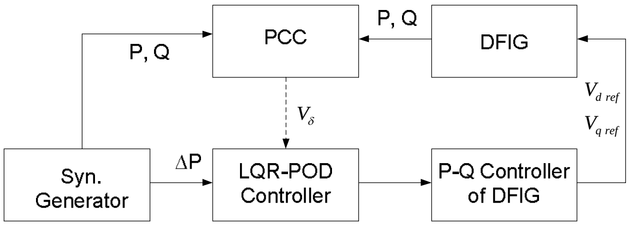

Figure 6. Proposed LQR-SSR controller for DFIG-Synchronous Generator

V. Simulation Results And Discussion

In this paper, the following cases has been examined which have a compensation of 50% and 60%.
Case A: The overall base system with DFIG.
Case B: The system in Case A is provided with a control signal derived from the synchronous generator.
Case C: The system in Case A is provided with a control signal derived from the synchronous generator, which is regulated by a LQR controller.
Two subcases with series compensation levels of 60% and 50% are tested for each of the cases. Utilising this specific level of compensation is necessary to activate various synchronous generator torsional modes. The work's goals are to do eigenvalue analyses for each of the aforementioned instances and to look into how the DFIG active and reactive power control technique with series compensation affects SSR. The evaluations of eigenvalues for the first scenario are shown in Table 2 in order to pinpoint the torsional modes with oscillation frequencies in the sub-synchronous range.
The positive real portion of a few torsional modes that are responsible for the system's subsynchronous resonance is highlighted. In contrast to the base system, the use of a Doubly Fed Induction Generator (DFIG) in conjunction with a transient active power regulation technique, using derived control signals from synchronous generators, has the potential to improve a specific torsional mode. However, it is important to note that this approach does not achieve total suppression of Subsynchronous Resonance (SSR). Although the torsional mode can be improved with the adoption of the DFIG power control method, the system's damping was insufficient.
The use of derived control signals from synchronous generators with LQR has been investigated as a way to lessen the effects of SSR and to achieve system stabilisation via the use of series compensation. Table 3 shows that using generator power deviation with LQR as an additional signal can effectively mitigate all torsional modes and stabilise the system. Even with a 60% or 50% degree of correction, all eigenvalues have negative real portions and lead to increased damping.

TABLE II. Results of Eigen Value Analysis For Case A

Series compensation level =60%	Series compensation level =50%	Oscillation Modes
0.000± 296.97i	-0.09± 293.97i	Torsional mode of synchronous generator
-0.007 ± 202.564i	-0.152 ± 203.16i	
-0.019 ± 156.74i	-0.153 ± 161.23i	
0.143 ± 126.798i	**0.186 ± 127.01i**	
0.398 ± 99.000i	-0.05 ± 98.85i	

TABLE III. Results of Eigen Value Analysis For Case B and Case C

CASE B		CASE C		Oscillations Modes
Percentage of Series Compensation		Percentage of Series Compensation		
60%	50%	60%	50%	
-0.001± 296.14i	-0.001± 298.74i	-0.008± 298.45i	-0.014± 295.47i	Torsional mechanical mode of synchronous generator
-0.007 ± 199.55i	-0.009 ± 201.51i	-0.032 ± 203.06i	-0.045 ± 201.87i	
-0.015 ± 162.52i	-0.021 ± 160.02i	-0.055 ± 165.15i	-0.078 ± 160.64i	
0.120 ± 125.97i	-0.023 ± 126.21i	-0.056 ± 122.16i	-0.049 ± 126.81i	
0.000 ± 99.510i	**0.124 ± 99.510i**	-0.009 ± 96.37i	-0.045 ± 98.81i	

Using derived equations, simulations in the time domain are also performed for cases B and C at a compensation level of 60% in MATLAB-Simulink. Figs. 7 and 8 demonstrate the time domain responses of the torque provided by the shaft between the LPA and LPB turbines of generator 1 and the mass oscillations for cases B and C, respectively, when the disturbance is delivered at t = 6 seconds. Time domain simulation findings confirm the outcomes of the analysis done of eigenvalues.

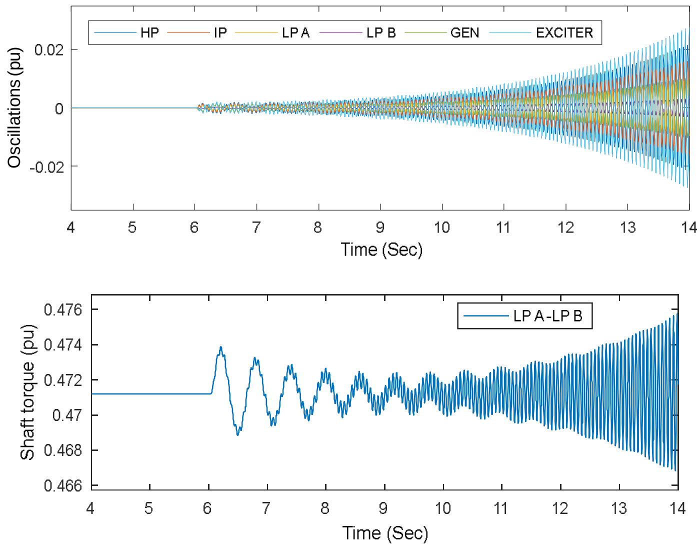

Figure 7. Oscillations Exhibited by Various Masses and Resulting Torque Exerted on LPA-LPB Shaft of a Generator, For Case B.

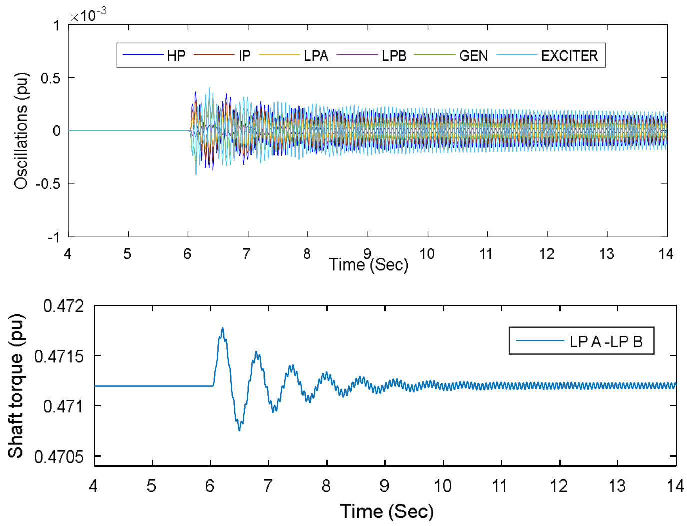

Figure 8. Oscillations Exhibited by Various Masses and Resulting Torque Exerted on LPA-LPB Shaft of a Generator, For Case C.

VI. Conclusion

This work uses state space modeling of different electrical components collected from IEEE FBM to investigate the impact of a power flow controller with LQR on subsynchronous resonance (SSR) in the selected test system. The occurrence of subsynchronous resonance (SSR) may be attributed to the presence of a series capacitor in a transmission network that is equipped with a certain amount of compensation. This study presents a systematic method to transient modeling of Doubly Fed Induction Generators (DFIG) with variations in the active and reactive power control loop. The modeling process incorporates varied component models to accurately represent the system dynamics. Two alternative compensation levels, 50% and 60%, are regarded as the most exciting modes for the turbo generator. According to eigenvalue analysis and time domain simulation, the DFIG cannot successfully dampen all of the generator's torsional oscillations when it is used with only its power control loop and a supplementary signal from the synchronous generator. When the Doubly Fed Induction Generator (DFIG) is used in combination with Linear Quadratic Regulator (LQR) and an extra signal derived from the power oscillation of the turbo generator, it is possible to dampen all torsional modes. This holds true even when the compensation level matches the natural frequency of the turbine-generator system.

REFERENCES

[1] IEEE Committee Report, “Readers Guide to subsynchronous resonance”, IEEE Trans. Power System, vol. 7, pp. 150-157, Feb-1992
[2] Kundur P, Power System Stability and Control, New Delhi: McGraw Hill, 2012
[3] P.M. Anderson, B.L. Agrawal, and J.E. Van Ness, Subsynchronous resonance in power systems (1st ed.). New Jersey: Wiley-IEEE Press. 1999
[4] IEEE SSR Working Group, “Countermeasures to subsynchronous resonance problems”, IEEE Transactions on Power Apparatus and Systems, vol. PAS-99, pp. 1810-1818. Sept. 1980
[5] Z. Rui, Li Gen and J. Liang, “Capability of TCSC on SSR mitigation”, Journal of Power and Energy Engineering, vol. 03, pp. 232-239. Jan. 2015.
[6] N. A. Patel and P. Bhatt, “SSR mitigation in power system with static synchronous series compensator”, International Journal of Engineering and Technology, vol. 3, pp. 1457-1462, July- 2018.
[7] N. A. Patel and P. Bhatt, “Mitigation of sub-Synchronous resonance with static var compensator”, Journal of Engineering Science and Technology, vol. 14, pp. 1101-1117, April-2019.
[8] X. Xie, H. Liu and Y. Han, “Coordinated design of supplementary excitation damping controller and voltage-sourced converter based generator terminal subsynchronous damping controller for subsynchronous resonance suppression: A case study”, Electrical Power Components and System, vol. 44, pp. 565-577, Feb. 2016.
[9] M. R. Patel and N. A. Patel, “Enhancement of transient stability on power system with The use of power system stabilizer”, International Conference on Electrical, Electronics, and Optimization Techniques (ICEEOT), Chennai, India, (2016), March 3-5, 2016.
[10] N. A. Patel and M R Patel, “Analysis of SSR with interplant power-flow controller”, Journal of Xidian University, Vol. 14, pp. 15-22, April 2020.
[11] N. A. Patel and M R Patel, “Mitigation of SSR in power system through power control of additional DFIG”, International Journal of Grid and Distributed Computing (IJGDC), vol. 13, no.1, pp. 851-859, May 2020.
[12] K. Kerrouche, A. Mezouar, and Kh. Belgacem, "Decoupled control of doubly fed induction generator by vector control for wind energy conversion system,” Energy Procedia, vol.42, pp. 239-248, 2013.
[13] R. Cárdenas, R. Peña, S. Alepuz, and G. Asher, “Overview of control systems for the operation of DFIGs in wind energy applications,” IEEE Transactions on Industrial Electronics, vol. 60, no. 7, pp. 2776–2798, July 2013.
[14] G. D. Marques, and D. M. Sousa, “New sensorless rotor position estimator of a DFIG based on torque calculations-stability study,” IEEE Transactions on Energy Conversion, vol. 27, no.1, pp. 196–203, March 2012.
[15] R. Datta and V. Ranganathan, “Direct Power Control of Grid-Connected wound rotor Induction Machine without Rotor Position Sensors”. IEEE Transactions on Power Electronics, vol. 16, pp. 390-399. May 2001.
[16] P.C. Krause, O. Wasynczuk and S.D. Sudhoff, Analysis of Electric Machinery and Drive Systems (2nd ed.). New Jersey: Wiley-IEEE Press, 2002.